

# Rapid Enrichment and Detection of Silk Residues from Tombs by Double-Antibody Sandwich ELISA Based on Immunomagnetic Beads

Hailing Zheng,\* Hailiang Yang, Yang Zhou,\* Tianxiao Li, Qinglin Ma, Bing Wang, Qin Fang, and Haixiang Chen



Cite This: <https://doi.org/10.1021/acs.analchem.1c02556>



Read Online

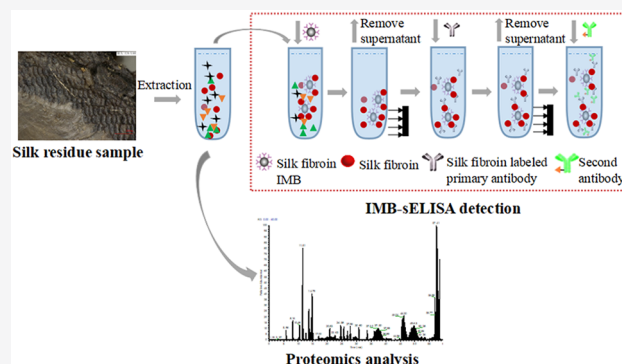
ACCESS |

Metrics & More

Article Recommendations

Supporting Information

**ABSTRACT:** The extraction and identification of silk residues in tombs is of great significance for studying the distribution and spread of early silk. However, the complex organic matter in the tomb hinders the accurate identification of silk. In this study, a double-antibody sandwich enzyme-linked immunosorbent assay (ELISA) based on immunomagnetic beads (IMBs) was developed for the rapid enrichment and detection of silk residues. The double-antibody sandwich ELISA method established by pairing the IMBs prepared by the silk fibroin monoclonal antibody SF-3 and the silk fibroin monoclonal-labeled antibody bio-SF-1 had the highest detection sensitivity, with a linear detection range of 10 to 10<sup>4</sup> ng mL<sup>-1</sup> and a detection limit of 5.12 ng mL<sup>-1</sup>. This method was excellent in the extraction and analysis of silk residues from archaeological imprints and soil samples and successfully identified silk residues in samples at the final stage of silk degradation (physical invisible silk). The proteomics analysis results demonstrated the feasibility and practicability of this method.



## INTRODUCTION

Silk is a kind of protein material that is very susceptible to aging and degradation due to environmental influences. According to the unearthed state of silk relics, they can be divided into physical silk fabric, carbonized silk fabric, mineralized silk fabric, and soil samples. Carbonized silk fabric, mineralized silk fabric, and soil samples are different from physical silk fabric and present limited residual information, although some material information will remain in bronze, soil, and other media. Currently, two methods are used for the identification of protein organic residues: proteomics methods and immunological techniques. Proteomics uses mass spectrometry or tandem mass spectrometry to identify the polypeptide sequence of the sample after protease digestion, and then a protein database search and homology comparison are performed to determine the source of the polypeptide according to the sequence and identify the protein components in the sample.<sup>1</sup> This method has confirmed the presence of proteins in relic samples, such as red makeup pens from the Xiaohe Cemetery in the Bronze Period,<sup>2</sup> bread from the Subeixi Cemetery buried 2500 years ago,<sup>3</sup> archaeological ceramic fragments,<sup>4</sup> and Huangwei from the Western Zhou Dynasty Cemetery.<sup>5</sup>

The immunological technique combines the sensitivity of enzymatic chemical reactions and the specificity of antigen–antibody reactions, which make it a sensitive and specific detection method.<sup>6</sup> This method has the advantages of rapid

detection, high sensitivity, simple operation, and low cost,<sup>7</sup> and it has been rapidly developed and widely used in the field of analysis and detection of ancient protein residues, including the detection of blood, collagen, egg white, and milk in stoneware and pottery residues, adhesives in murals and lacquer, silk protein residues in tombs, and so forth.<sup>8–14</sup>

The sources of protein in tombs are complex, including degradation products of human protein, microorganisms, and animal fibers, which can easily interfere with the fine identification of residues. The proteomics analysis process is very complicated and includes the dissolution, extraction, concentration, enzyme digestion, and mass spectrometry analysis of the target components. The extraction and concentration of the target components determine the accuracy of the mass spectrometry results. Antigen–antibody reactions require the target protein to be purified or separated from ancient fabric imprints or soil before the reaction. Fabric imprints and soil have a complex composition and low effective content of target components. Thus, determining a method of enriching and extracting the target protein from a large number

**Received:** June 17, 2021

**Accepted:** September 22, 2021

of archaeological collections is critical to the success of the test. Immunomagnetic beads (IMBs) which can enrich and purify silk protein in solution were prepared by coupling silk protein antibody with magnetic beads. Then, the indirect enzyme-linked immunosorbent assay (ELISA) was used to evaluate the enrichment effect of the IMBs.<sup>15</sup> This process involves the elution of silk protein on the IMBs and presents the problems of insufficient elution and complicated operations. For samples with trace amounts of protein, such as soil from archaeological sites, if the elution is insufficient, the test results will be affected.

In the present study, a method based on sandwich ELISA detection and IMB enrichment for rapid enrichment and detection of silk fibroin in tombs was developed. The magnetic beads are coupled with monoclonal antibodies to form a solid-phase carrier and then combined with the double antibody sandwich method to quickly separate and detect trace silk proteins in textile imprint samples and soil samples. Proteomics was subsequently used to further confirm the detection results. For the identification of silk residue samples (physical invisible silk), immunological technology combined with proteomics can accurately identify its components and sources.

## MATERIALS AND METHODS

**Materials and Instruments.** Carboxyl magnetic beads were purchased from Enriching Biotechnology Ltd, China. Bovine serum albumin (BSA), iodoacetamide (IAA), sodium lauryl sulfate (SDS), acetone, tris(hydroxymethyl)-amino-methane hydrochloride (Tris-HCl), and ammonium bicarbonate ( $\text{NH}_4\text{HCO}_3$ ) were purchased from Sigma-Aldrich. We prepared silk fibroin monoclonal antibodies (SF-1, SF-2, SF-3, SF-4, and SF-5) and obtained SA-HRP goat anti-mouse secondary antibody and 96-well enzyme plates from Hangzhou Hua'an Biotechnology Co., Ltd. Silk fibroin monoclonal antibodies can be used by researchers in the field of heritage, and the process of their preparation is presented in [Supporting Information S-2](#). Morpholine ethanesulfonic acid (MES) was purchased from McLean Biochemical Technology Co., Ltd. 1-Ethyl-(3-dimethylaminopropyl) carbon diimide hydrochloride (EDC) and tetramethyl benzidine (TMB) were purchased from Aladdin Chemical Co., Ltd. Phosphate-buffered saline (PBS) (pH = 7.4) was prepared with  $\text{KH}_2\text{PO}_4$ ,  $\text{Na}_2\text{HPO}_4$ , NaCl, and KCl. Coupling buffer was prepared with EDC and MES. Coating buffer (pH = 9.6) was prepared with  $\text{Na}_2\text{CO}_3$  and  $\text{NaHCO}_3$ . The stopping solution was concentrated  $\text{H}_2\text{SO}_4$  diluted to a 2 M solution. Trypsin was supplied by Promega Biotech Co., Ltd. (Beijing). Formic acid (FA), acetonitrile (ACN), and dithiothreitol (DTT) were purchased from Thermo Fisher Scientific.

A magnetic separation rack was purchased from Enriching Biotechnology Ltd., China. A centrifuge (TG16-WS) was purchased from Shanghai Luxiang Instrument Co., Ltd., China. A dancer shaker was purchased from Ningbo Qun'an Experimental Instrument Co., Ltd., China.

### Detection of the Preservation State of Relic Samples.

The cultural relic samples are shown in [Figure 1](#). Sample I (CX0045-1) came from the Han Tomb in Changxing, Zhejiang Province, and is currently housed at the Zhejiang Institute of Cultural Relics and Archaeology. The organic matter in the coffin of the tomb was completely decayed, and only inorganic cultural relics, such as copper coins and soil, remained at the bottom of the coffin. The soil samples near the



**Figure 1.** Images of cultural relics: (I) soil sample from the Han Tomb of Changxing, Zhejiang Province, and (II) soil sample with a fabric imprint from tomb no. 88 at the Sujialong site.

coins were extracted for experiments. Sample II (M88@E33N6) came from Tomb 88 of the Sujialong site and is currently housed at the Hubei provincial museum. The owner of Tomb 88 was Mi Ke of Chu State. The tomb was buried under acidic soil in southern China for more than 3000 years. The bones of Mi Ke and the coffin were corroded and invisible to the naked eyes, a large number of jade artifacts were unearthed from the tombs, and fabric imprints were found on the partial soil layer of the tomb. Soil samples with fabric imprints were extracted for tests.

The morphologies of the relic samples were characterized by a three-dimensional microscope (VHX-2000C, Keyence, Japan) and a scanning electron microscope (Sigma 300, ZEISS, Germany). The scanning electron microscopy (SEM) was used to observe the longitudinal morphologies of the fibers and collect images at magnifications of 100 times to 2000 times.

To obtain the internal structure information of the imprint samples, three-dimensional X-ray microscopy (X-ray CT) was conducted using a ZEISS Xradia 610 (XRM). A sample of the appropriate size was collected and fixed on the support through a homemade device to ensure that it did not move during the rotation of the stage. Using an objective lens of 4 $\times$ , an imprint sample was scanned with an X-ray source voltage and power of 60 kV and 6.5 W, respectively. A total of 3001 projections were obtained, with a 3 s exposure time for each set, resulting in a total acquisition time of 3 h 55 min. Images were combined and reconstructed by image software to analyze the images of the three-dimensional structure of the samples and the phase composition of the sample.

**Extraction of Silk Fibroin.** Modern silk samples were extracted as previously reported,<sup>16,17</sup> and silk fibroin was extracted with  $\text{CaCl}_2$  ethanol solution ( $\text{CaCl}_2$ /ethanol/water molar ratio of 1:2:8). The process included degumming, dissolution, dialysis, filtration, and freeze-drying. Finally, the fibroin powder was stored at  $-20^\circ\text{C}$  for further experiments.

Certain amounts of samples I and II were crushed and then dissolved in the silk fibroin extraction solution ( $\text{Na}_2\text{CO}_3$  1.5 g,  $\text{NaHCO}_3$  2.9 g, added  $\text{H}_2\text{O}$  to 1000 mL) with a bath ratio of 1:50 at  $90 \pm 2^\circ\text{C}$  for 30 min.<sup>18</sup> Then, the supernatant was centrifuged and extracted for subsequent experiments.

### Preparation and Labeling of Monoclonal Antibodies.

Five monoclonal antibodies (SF-1, SF-2, SF-3, SF-4, and SF-5) were developed in the mice through immunization, cell fusion, and purification. The SF-3 monoclonal antibody had the highest titer and was selected for the preparation of IMBs,<sup>19</sup> and the four monoclonal antibodies SF-1, SF-2, SF-3, and SF-5 were labeled with biotin, and the process of labeling antibodies is presented in the [Supporting Information S-3](#). The optimum

dilution ratio of the labeled monoclonal antibody was selected by indirect ELISA detection steps as previously reported.<sup>19</sup> Silk fibroin solution (1  $\mu\text{g}/\text{mL}$ ) and BSA solution (1  $\mu\text{g}/\text{mL}$ ) were prepared for antibody titer detection. The labeled monoclonal antibody was diluted at 1:1000, 1:2k, 1:5k, 1:25k, 1:125k, 1:625k, and 1:325k, and the SA-HRP antibody diluted to 1:3000 was selected for the secondary antibody. According to the results of indirect ELISA detection, the selected dilution ratios of the bio-SF-1, bio-SF-2, bio-SF-3, and bio-SF-5 antibodies were 1:2000, 1:1000, 1:2000, and 1:1000 for antibody pairing.

**Detection of Paired Sensitivity of Monoclonal Antibodies.** Silk protein monoclonal antibodies were diluted with coating buffer in different proportions, the SF-1, SF-2, and SF-5 antibodies were diluted at 1:2000, and the SF-3 antibody was diluted at 1:4000.<sup>15</sup> Fifty microliters of the silk protein monoclonal antibody solution was added to each well. For the blank control group, 50  $\mu\text{L}$  of coating buffer was directly added to each well, the microtiter plate was coated at 4  $^{\circ}\text{C}$  overnight, and 300  $\mu\text{L}$  of PBS was subsequently added to each well for washing, which was repeated three times. Then, 200  $\mu\text{L}$  of 1% BSA solution was added to each well and incubated for 1 h at 37  $^{\circ}\text{C}$ , and 300  $\mu\text{L}$  of PBS was subsequently added to each well for washing, which was repeated three times. The silk fibroin was dissolved and diluted with PBS (concentrations were 0, 12.5, 25, 50, 100, 200, 400, and 800  $\text{ng}/\text{mL}$ ). PBS was used as the control group. Silk protein solution (50  $\mu\text{L}/\text{well}$ ) and PBS were added to the microtiter plate and incubated at 37  $^{\circ}\text{C}$  for 1 h. After washing with 300  $\mu\text{L}/\text{well}$  of PBS three times, 50  $\mu\text{L}/\text{well}$  of labeled primary antibody diluted with 0.1% BSA in PBS was added to the microtiter plate and reacted at 37  $^{\circ}\text{C}$  for 30 min. Then, the plate was washed with PBS three times. 50  $\mu\text{L}/\text{well}$  of secondary antibody diluted with 0.1% BSA in PBS (1:5000) was then added to the microtiter plate and reacted at 37  $^{\circ}\text{C}$  for 30 min. After washing (as above), 100  $\mu\text{L}$  of TMB solution was added away from the light and reacted at room temperature for 5 min. Finally, 50  $\mu\text{L}/\text{well}$  of stop solution was added, and the optical densities ( $\text{OD}_{450\text{nm}}$ ) were measured with a microplate detector (iMark, Bio-Rad, USA).

**Preparation of IMBs.** As previously reported,<sup>15</sup> the SF-3 monoclonal antibody and magnetic beads were used to prepare IMBs. Carboxyl magnetic beads were washed with deionized water and 100 mM MES solution, and then the SF-3 monoclonal antibody was added to react with them for 30 min. Subsequently, EDC solution was added to react for 2 h, and then TT buffer was added and incubated with the reacted MBs at room temperature for 1 h. After magnetic separation and washing, the IMBs were resuspended in BSA dissolved in PBS to block excess reactive sites. Finally, IMBs were washed and resuspended in PBS buffer containing 0.02%  $\text{NaN}_3$  for further experiments.

**Establishment of the IMB-sELISA Method.** Several copies of 50  $\mu\text{g}$  IMBs that had been blocked with 500  $\mu\text{L}$  of blocking solution were added to separate centrifuge tubes, washed twice with 200  $\mu\text{L}$  PBS, and placed in tubes in the magnetic separation rack to separate and carefully remove the supernatant. The silk fibroin solution was diluted in gradients, and 200  $\mu\text{L}$  of each gradient was added to the centrifuge tube. The reaction was carried out at 37  $^{\circ}\text{C}$  for 1 h, and the IMBs were shaken every 10 min. After magnetic separation and washing three times with PBS, 200  $\mu\text{L}$  of primary antibody diluted with 0.1% BSA in PBS was added to a centrifuge tube and reacted at 37  $^{\circ}\text{C}$  for 30 min. After removing the

supernatant and washing with PBS, 200  $\mu\text{L}$  of secondary antibody SA-HRP diluted with 0.1% BSA in PBS was added to the centrifuge tube and reacted at 37  $^{\circ}\text{C}$  for 30 min. Then, after magnetic separation and washing with PBS, 100  $\mu\text{L}$  of TMB solution was added to the centrifuge tube and placed at 37  $^{\circ}\text{C}$  away from the light for 5 min. For magnetic separation, the liquid was extracted and added to the ELISA plate, and 50  $\mu\text{L}/\text{well}$  stopping solution was added to terminate the reaction. Finally, the  $\text{OD}_{450\text{nm}}$  was detected.

**Proteomics Analysis.** Samples I and II were subjected to drying and concentration, respectively. After concentration, an appropriate amount of SDT lysis solution (4% SDS, 100 mM DTT, and 100 mM Tris-HCl) was added to the samples, which were then heated in a boiling water bath for 5 min and cooled to room temperature. IAA (50 mM) was then added to the samples, which were shaken at 600 rpm for 1 min, and the reaction was performed at room temperature in the dark for 30 min. Then, 6 times the volume of cold acetone was added and placed at  $-20$   $^{\circ}\text{C}$  for 2 h to precipitate the protein, and the supernatant was removed after centrifugation at 16,000g for 10 min. Acetone was added to clean the protein precipitates, and the process was repeated twice. Then, the protein precipitates were digested with 100  $\mu\text{L}$  of trypsin buffer (2  $\mu\text{g}$  trypsin in 100  $\mu\text{L}$  of  $\text{NH}_4\text{HCO}_3$  buffer) for 16–18 h at 37  $^{\circ}\text{C}$ , and the resulting peptides were collected by centrifugation. The peptides of each sample were desalted on C18 and dried under vacuum. Finally, the peptides were resuspended in 0.1% FA for the liquid chromatography (LC)–mass spectrometry (MS) analysis.

An appropriate amount of peptides from each sample was separated under a 60 min B liquid (0.1% FA, 80% ACN and  $\text{H}_2\text{O}$ ) gradient (2–100%) in 0.1% FA at a nanoliter flow rate with a Thermo Scientific EASY-nLC 1200 system, and the detailed gradient information is listed in [Supporting Information S-4](#). A Q-Exactive HF-X mass spectrometer was directly operated to analyze the separated peptides in the data-dependent acquisition mode. MaxQuant 1.6.1.0 software was used to compare the original data with 18,488 protein sequences of *Bombyx mori* downloaded from the UniProt Protein Database. The search contained fixed modifications of carbamidomethyl and dynamic modifications of N-terminal acetyl and methionine oxidation. The precursor tolerance was set to 20 ppm, with a maximum of two missed cleavages allowed.

## RESULTS AND DISCUSSION

**Preservation State of Relic Samples.** The three-dimensional images of relic samples are shown in [Figure 2](#).



**Figure 2.** Three-dimensional image of the relic sample: (I) soil sample from the Han Tomb of Changxing, Zhejiang Province, and (II) soil sample with a fabric imprint from Tomb no. 88 at the Sujialong site.

The surface of sample I, which was soil, had no fabric information. The surface of sample II clearly shows fabric residual imprints, and imprints with a convex–concave surface were arranged continuously similar to a plain weave. The fibers were degraded into the imprints after aging and hence lost their shape. As shown in the SEM images (Figure 3), there

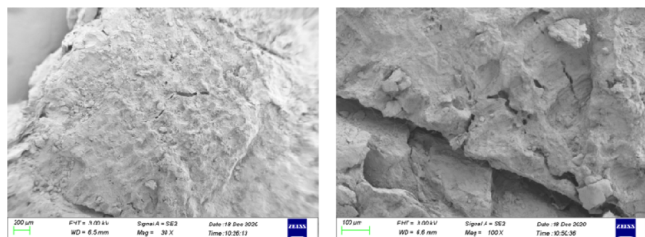


**Figure 3.** SEM images of the fabric imprint from Tomb 88 of the Sujialong site.

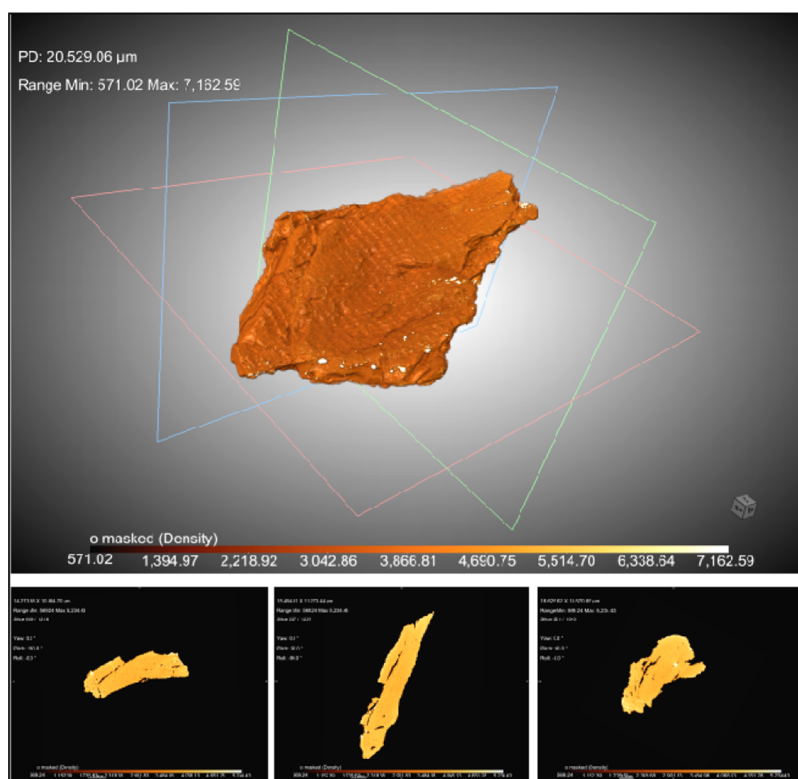
were no residual fibers on the surface of the imprints, which indicated that the fabric had been completely degraded. In this state, conventional spectral analysis methods and morphological methods can no longer be used to identify the fiber material of the fabric.<sup>20,21</sup>

The 3D reconstruction of the fabric imprint is presented in Figure 4. Figure 4a–c presents the internal cross-sectional structure of the imprint sample. The grayscale of the image corresponds to the X-ray absorption coefficient of the substance, and different phases can be distinguished according to the absorption coefficient; thus, the composition of different phases can be clearly observed through three-dimensional rendering.<sup>22,23</sup> Figure 4 shows that the surface of the imprint

sample had only one phase, and its internal cross-sectional structure showed the same state, which indicated that the density of the fabric imprint was close to the density of the soil beneath the imprint and the fabric had been completely soiled.

**Sensitivity of the Paired Antibodies.** The double-antibody sandwich ELISA test results of paired antibodies are shown in Table 1. The results showed that the OD value of the PBS group (without antigen) was lower (OD value < 0.2), and the paired background was also lower. Among the 11 pairs of antibodies, SF-1 and bio-SF-3, SF-2 and bio-SF-2, and SF-3 and bio-SF-1 were the best-paired groups.

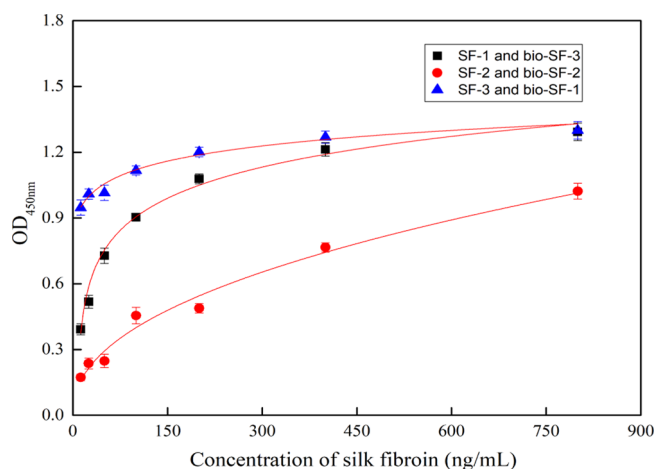
To evaluate the sensitivity of the three groups of paired antibodies, the silk protein concentration was used as the X-axis and the OD<sub>450nm</sub> value was used as the Y-axis for the curve fitting analysis. The cutoff was defined as 2.1 times the mean OD<sub>450nm</sub> of the negative control. Substituting the cutoff value into the regression equation, the limit concentration could be obtained. As shown in Figure 5, the regression equation of SF-1 and bio-SF-3 was  $y = 0.198 \ln(x - 6.031)$  ( $R^2 = 0.9884$ ), the cutoff value was 0.2625, and the limit concentration was calculated as 27.215 ng/mL. The regression equation of SF-2 and bio-SF-2 was  $y = 0.051x^{0.449}$  ( $R^2 = 0.980$ ), as shown in Figure 6. The cutoff value was 0.334, and the limit concentration was calculated as 68.845 ng/mL. The regression equation of SF-3 and bio-SF-1 was  $y = 0.832 + 0.069 \ln(x - 10.424)$  ( $R^2 = 0.997$ ), as shown in Figure 7. The cutoff value was 0.529, and the limit concentration was calculated as 10.425 ng/mL. In comparison, the detection sensitivity of the SF-3 and bio-SF-1 double-antibody sandwich ELISA was the highest. Therefore, SF-3 and bio-SF-1 were used to construct the sandwich ELISA method of IMB double antibodies.



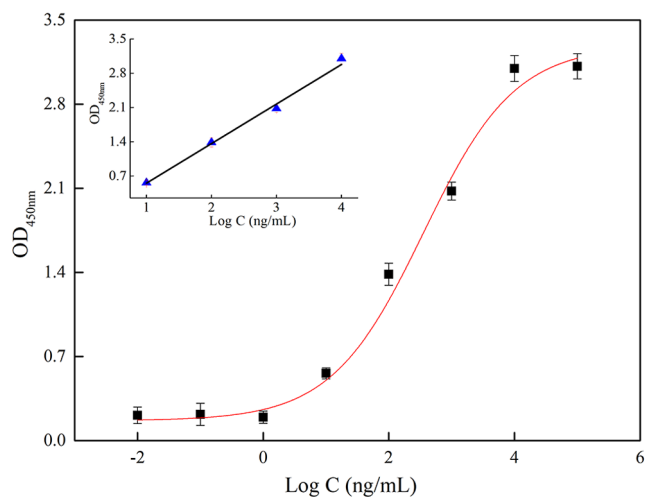
**Figure 4.** 3D CT reconstruction and rendering of the fabric imprint from Tomb 88 at the Sujialong site. Details (a–c) present CT slices (along the XZ, XY, and YZ directions, respectively) showing the internal cross-sectional structure of the imprint sample.

Table 1. Results of the Double-Antibody Sandwich ELISA Test

	SF-1		SF-2		SF-3		SF-5	
	bio-SF-3	bio-SF-5	bio-SF-2	bio-SF-5	bio-SF-1	bio-SF-2	bio-SF-5	bio-SF-5
800 ng/mL	1.293 ± 0.04	0.884 ± 0.029	1.022 ± 0.036	0.564 ± 0.026	1.3 ± 0.040	0.722 ± 0.025	0.415 ± 0.020	0.422 ± 0.017
400 ng/mL	1.213 ± 0.031	0.75 ± 0.025	0.766 ± 0.021	0.408 ± 0.015	1.269 ± 0.028	0.591 ± 0.023	0.388 ± 0.018	0.294 ± 0.012
200 ng/mL	1.078 ± 0.022	0.628 ± 0.021	0.488 ± 0.022	0.337 ± 0.012	1.201 ± 0.022	0.50 ± 0.021	0.337 ± 0.015	0.268 ± 0.015
100 ng/mL	0.903 ± 0.018	0.511 ± 0.023	0.455 ± 0.038	0.264 ± 0.018	1.117 ± 0.021	0.461 ± 0.011	0.322 ± 0.018	0.197 ± 0.012
50 ng/mL	0.728 ± 0.035	0.451 ± 0.028	0.248 ± 0.030	0.235 ± 0.020	1.015 ± 0.035	0.391 ± 0.015	0.232 ± 0.010	0.196 ± 0.013
25 ng/mL	0.518 ± 0.029	0.321 ± 0.021	0.236 ± 0.025	0.203 ± 0.011	1.009 ± 0.024	0.295 ± 0.012	0.219 ± 0.012	0.172 ± 0.019
12.5 ng/mL	0.392 ± 0.025	0.246 ± 0.024	0.173 ± 0.015	0.199 ± 0.014	0.947 ± 0.035	0.274 ± 0.013	0.185 ± 0.014	0.168 ± 0.010
PBS	0.125 ± 0.015	0.124 ± 0.012	0.159 ± 0.014	0.129 ± 0.010	0.252 ± 0.020	0.149 ± 0.013	0.136 ± 0.012	0.148 ± 0.013



**Figure 5.** Fitting line of SF-1 and bio-SF-3, SF-2 and bio-SF-2, and SF-3 and bio-SF-1 double-antibody sandwich ELISA tests. The error bars represent the error value of five parallel experiments under each experimental condition of the double-antibody sandwich ELISA.



**Figure 6.** Standard curve of IMB-sELISA for the detection of silk fibroin. The error bars represent the error value of five parallel experiments under each experimental condition of IMB-sELISA to detect silk fibroin.

**Standard Curve of IMB-sELISA for Detection of Silk Fibroin.** The silk fibroin solution was diluted at a concentration of  $10^{-2}$  to  $10^6$  ng/mL and used for IMB-sELISA detection. With increasing concentration, the  $OD_{450nm}$  gradually increased. Taking the silk protein logarithmic concentration as the X-axis and the corresponding  $OD_{450nm}$  value as the Y-axis, the curve was in the shape of an “S” (Figure 6). When the silk fibroin concentration was 10 to  $10^4$  ng/mL, the silk fibroin concentration had a good linear relationship with the  $OD_{450nm}$  value. A linear fit was performed on this range, and the linear equation was  $y = 0.81x - 0.256$  ( $R^2 = 0.9933$ ), the cutoff value was 0.317, and the limit concentration was calculated as 5.12 ng/mL. The results showed that the detection limit of this method was lower than that of double-antibody sandwich ELISA, which indicated that the IMBs efficiently concentrated the silk protein, which is beneficial for subsequent detection.

IMB-sELISA detection of silk protein in simulated soil samples was performed. Soil samples were collected approx-

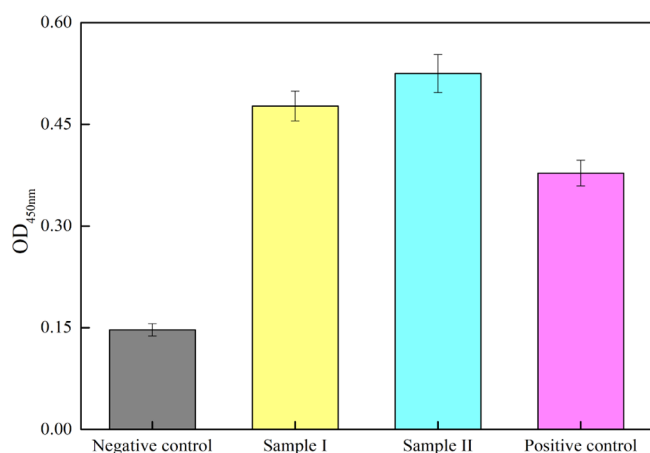


**Figure 7.** IMB-sELISA results for sample I and sample II. BSA as a negative control, and silk fibroin as a positive control. The dotted line in the figure represents the limit value used to judge the experimental results, which is positive above the dotted line value and negative below it. The error bars represent the error value of four parallel experiments under each experimental condition of IMB-sELISA.

imately 10 cm below the ground, dried at 60 °C, and crushed, and after removing the impurities, they were stored for later use. One milligram of silk fibroin was weighed and diluted with deionized water  $10^4$ ,  $10^3$ ,  $10^2$ , and 10 times (the corresponding concentrations were  $10^1$ ,  $10^2$ ,  $10^3$ , and  $10^4$  ng/mL, respectively). Then, 1 mL of silk fibroin solution and 0.01 g of soil samples were removed and mixed (the proportion of silk fibroin in the soil samples was  $10^{-4}$ ,  $10^{-3}$ ,  $10^{-2}$ , and  $10^{-1}\%$ ) and placed in an oven at 50 °C for 3 days until no moisture remained. The samples were removed and cooled to room temperature, and then four portions of 1 mL of silk fibroin extraction solutions ( $\text{Na}_2\text{CO}_3$  1.5 g,  $\text{NaHCO}_3$  2.9 g, added  $\text{H}_2\text{O}$  to 1000 mL) were added to each soil sample and evenly stirred and centrifuged. Then, the supernatant was collected for IMB-sELISA detection. The linear equation in Figure 6 was used to calculate the content of silk fibroin in each soil sample component. The quantitative results showed that when the concentrations were  $10^1$ ,  $10^2$ ,  $10^3$ , and  $10^4$  ng/mL, the detection results were 9.33, 89.11, 843.72, and 7833.69 ng/mL, respectively. This finding indicates that when the IMB-sELISA method is applied to soil samples, the impurities in the soil will lead to a lower detection value than the actual value. However, this discrepancy may also be because silk fibroin binds together with a certain force in the soil sample to form soil organic aggregates,<sup>24,25</sup> which increases the difficulty of completely extracting the proteins. Moreover, complex impurities in the soil will also adhere to the surface of the magnetic beads, resulting in fewer binding sites between the silk fibroin and IMBs. These influencing factors have a limited impact on the sensitivity of IMB-sELISA, which presents high sensitivity in soil samples; in addition, the expected results will

likely be obtained by applying this method to relic imprinted and soil samples.

**IMB-sELISA Detection of Relic Samples.** The established IMB-sELISA was applied to the detection of cultural relic samples. As shown in Figure 7, sample I and sample II gave positive results, indicating that both soil samples contained silk protein residues, and the concentrations calculated from the linear equation in Figure 6 were 8.02 and 9.20 ng/mL, respectively. The results demonstrated that the IMB double-antibody sandwich ELISA is an effective and simple method for qualitative and quantitative analyses of soil samples and is superior to other chemical methods, which cannot achieve sample enrichment and detection at the same time.

**Proteomics Analysis of Relic Samples.** Tables 2 and 3 show the LC-MS/MS test results of the Han Dynasty soil sample from Anji and the textile imprint sample from the Sujialong site, respectively. Four silk proteins were detected in the soil samples from the Han Dynasty tomb in Anji, and they were all functional proteins. Thirty-eight silk proteins were detected in the textile imprint samples from the Sujialong site, 19 of which were functional proteins. According to the test results, it can be judged that both cultural relic samples contain silk protein. A symbolic protein of *B. mori* silk numbered P05790<sup>26,27</sup> was detected in two samples, and it belongs to the *B. mori* silk heavy chain proteins. It was confirmed that the silk proteins in the two samples came from *B. mori* silk, which indicates that silk fabrics were present in both tombs. The proteomics analysis results are consistent with the IMB-sELISA results.

Silk products are easily degraded under the influence of humidity and microorganisms in the burial environment. Their degradation is not only affected by the burial time but also closely related to the burial environment.<sup>28</sup> The Anji Han Tomb was sealed more than 2200 years ago, and Tomb M88 of Sujialong was sealed more than 3000 years ago. The Anji Han Tomb is located on the southeastern coast of China, which has abundant rainfall. The tomb has been infiltrated by rain and is in a semidry and semiwet state, which has accelerated the aging and degradation of silk and other organic cultural relics. Therefore, the number of polypeptides that can be detected is significantly less than that of Tomb M88 of Sujialong. Compared with the proteomic analysis results of modern silk, the silk protein in these two cultural relic samples was in the final stage of degradation, and the heavy chain, light chain, and P25 chain were all degraded.<sup>16</sup> Thus, only a small number of polypeptide molecules were retained, and they were adsorbed by soil particles.<sup>29–33</sup>

## DISCUSSION

Silk fabrics are easily degraded, and there is little chance of discovering silk fabrics in the early archaeological sites. The earliest silk fabric found in China was the leno fabric unearthed in 1983 at the Yangshao Cultural Site in Qingtai Village,

**Table 2.** Identified Proteins in the Soil Sample of Han Dynasty from Anji

accession number	description	peptides	unique peptides	score	species
P05790	fibroin heavy chain	2	2	323.31	BOMMO
H9IVT4	ricin B-type lectin domain-containing protein	1	1	6.9406	BOMMO
J7ET58	methuselah-like protein 10	1	1	6.5139	BOMMO
H9JAX4	ubiquitinyl hydrolase 1	1	1	5.9911	BOMMO

Table 3. Identified Proteins in the Textile Imprint Sample from Sujialong

accession number	description	peptides	unique peptides	score	species
O16143	Rab1 protein	1	1	323.31	BOMMO
P05790	fibron heavy chain	3	3	318.55	BOMMO
SSM4F4	truncated actin-4	1	1	162.18	BOMMO
W6JHY5	homothorax	2	2	26.876	BOMMO
H9IZG4	TIP120 domain-containing protein	1	1	10.793	BOMMO
H9IUL0	CRAL-TRIO domain-containing protein	1	1	9.2616	BOMMO
H9J6M8	ANK_REP_REGION domain-containing protein	1	1	8.8994	BOMMO
H9JKZ4	delta-like protein	1	1	8.2448	BOMMO
W6AQJ8	DNA polymerase	1	1	8.2448	BOMMO
D0VEM7	putative cuticle protein	1	1	7.919	BOMMO
H9J493	THAP-type domain-containing protein	1	1	7.5353	BOMMO
H9JLP7	Rab-GAP TBC domain-containing protein	1	1	7.5353	BOMMO
H9JQ67	protein kinase domain-containing protein	1	1	7.5353	BOMMO
H9JRH4	E3 ubiquitin-protein ligase	1	1	7.5353	BOMMO
H9JW98	carboxylic ester hydrolase	1	1	6.192	BOMMO
Q75UA2	pyruvate kinase	1	1	5.8995	BOMMO
H9JS78	DZF domain-containing protein	1	1	5.735	BOMMO
B9X256	similar to poly(A)-specific ribonuclease, PARN	1	1	5.6511	BOMMO
H9JGR9	NOC3-like protein	1	1	5.6511	BOMMO

Xingyang City, Henan Province, dating back more than 5000 years.<sup>34</sup> Imprints and soil are the main carriers of early silk residues. Most of the remains unearthed from early archaeological sites, such as human bones, are in an open environment, and the burial objects have disappeared. The direct contact of external environment with the human body accelerates the degradation of silk fabric and the loss of silk fibroin, which results in low concentrations of the silk fibroin, especially in soil. The ELISA technology based on silk fibroin antibody has been applied to ancient silks, mineralized samples, and silt samples,<sup>14,18,19</sup> no matter which kind of sample is much more enriched than soil samples. For the soil samples from the early archaeological sites, even though a large number of experimental soil samples can be obtained, it is not possible to ensure that sufficient amount of silk fibroin can be extracted for ELISA detection. In this article, the IMB-sELISA detection method was constructed using silk fibroin monoclonal antibodies which developed in house. The specificity of monoclonal antibodies SF-1, SF-2, SF-3, and SF-5 was detected by indirect ELISA. The results showed that the SF-1, SF-2, SF-3, and SF-5 were only effective for *B. mori* silk and would not produce positive results for wool, linen, tussah silk, and castor silk.<sup>19</sup> This indicates that the IMB-sELISA detection method also has high specificity and can avoid false positive results in complex archaeological samples. This is extremely important for the identification of silk residues in soil samples. In the absence of physical evidence, this reliable identification method is needed.

The process of IMB enrichment, elution, and indirect ELISA detection takes at least 2 days because the microsamples need to be coated on an ELISA plate overnight. The detection process and results are listed in Supporting Information S-5. The same antibody SF-1 detected by IMB-sELISA was used as the primary antibody to identify silk fibroin. Comparing the experimental results, it was found that the two archaeological samples also showed positive results. The OD<sub>450nm</sub> value of sample I was 0.352 ± 0.015, and the OD<sub>450nm</sub> value of sample II was 0.475 ± 0.025, both of which were lower than the results of IMB-sELISA (Table S1). This is mainly due to the incomplete elution of silk fibroin during the elution of IMBs,

and the adsorption process of silk fibroin on the microtiter plate in the indirect ELISA detection may also cause some errors. In addition, the eluent methanol needs to be removed before ELISA detection. The whole experimental process is a bit complicated and time-consuming. The IMB-sELISA detection method avoids these problems and effectively improves the detection efficiency, and the entire experiment process only takes about 3 h. These advantages are very beneficial to the popularization and application of this method in the identification of historic residues.

The IMB-sELISA method and proteomics technology with two different technical principles were used to mutually verify the identification results of silk residues, which confirmed the applicability of IMB-sELISA method in the identification of trace silk residues. The analysis and detection of silk residues is expected to outline the origin area and time map of silk and also enable us to obtain more information to interpret ancient civilizations.

## CONCLUSIONS

The main challenge with using the established methods of IMB enrichment and immunological detection for archaeological samples is the low content of silk residues available in the tomb. After the enrichment of IMBs, silk protein elution is performed, followed by immunological detection. The complicated operation process will lead to a loss of silk protein. In this paper, a double-antibody sandwich ELISA based on IMBs was developed, and it can quickly enrich and detect silk residues in tombs. Silk residues of silk protein were detected in both imprint samples and soil samples extracted from the tombs, and the concentration calculated by this method was consistent with the proteomics analysis results. The residual silk protein information obtained for the imprint sample was greater than that obtained for the soil sample despite the sample having been completely soiled by X-ray CT scan. For the detection of silk residues in imprint samples, especially soil samples, the combination of immunological method and proteomics technology can ensure the accuracy of the detection results.

## ■ ASSOCIATED CONTENT

### SI Supporting Information

The Supporting Information is available free of charge at <https://pubs.acs.org/doi/10.1021/acs.analchem.1c02556>.

Details of experimental methods and results of indirect ELISA detection (PDF)

## ■ AUTHOR INFORMATION

### Corresponding Authors

**Hailing Zheng** – College of Textile Science and Engineer (International Institute of Silk), Zhejiang Sci-Tech University, Hangzhou 310018, China; China National Silk Museum, Hangzhou 310002, China; [orcid.org/0000-0003-3257-460X](https://orcid.org/0000-0003-3257-460X); Phone: +86-571-87035587; Email: 260974953@qq.com

**Yang Zhou** – China National Silk Museum, Hangzhou 310002, China; Email: 564949101@qq.com; Fax: +86-571-87068136

### Authors

**Hailiang Yang** – China National Silk Museum, Hangzhou 310002, China

**Tianxiao Li** – Joint International Research Laboratory of Environmental and Social Archaeology, Shandong University, Qingdao 266237, China

**Qinglin Ma** – Joint International Research Laboratory of Environmental and Social Archaeology, Shandong University, Qingdao 266237, China

**Bing Wang** – School of Materials Sciences & Engineering, Zhejiang Sci-Tech University, Hangzhou 310018, China; [orcid.org/0000-0002-3499-7828](https://orcid.org/0000-0002-3499-7828)

**Qin Fang** – Hubei Provincial Museum, Wuhan 430077, China

**Haixiang Chen** – School of Materials Sciences & Engineering, Zhejiang Sci-Tech University, Hangzhou 310018, China

Complete contact information is available at:

<https://pubs.acs.org/10.1021/acs.analchem.1c02556>

### Author Contributions

The manuscript was written through contributions of all authors. All authors have given approval to the final version of the manuscript.

### Notes

The authors declare no competing financial interest.

## ■ ACKNOWLEDGMENTS

We sincerely thank the Zhejiang Provincial Institute of Cultural Relics for providing the soil samples. We also thank Shanghai BioProfile Technology Company Ltd for technological assistance in proteomics experiment. H.Z., H.Y., and B.W. received funding from the National Natural Science Foundation of China (51803237). Y.Z. and H.Z. received funding from the National Key R&D Program of China (2019YFC1521302). T.L. and Q.M. received funding from the China Postdoctoral Science Foundation (2019M662390). H.Z. and B.W. received funding from the Special Funds from the Administration of Cultural Heritage of Zhejiang Province (2019004 and 2020012).

## ■ REFERENCES

(1) Hendy, J.; Welker, F.; Demarchi, B.; Speller, C.; Warinner, C.; Collins, M. J. *Nat. Ecol. Evol.* **2018**, *2*, 791–799.

(2) Mai, H.; Yang, Y. M.; Abuduresule, I.; Li, W. Y.; Hu, X. J.; Wang, C. S. *Sci. Rep.* **2016**, *6*, 18939.

(3) Shevchenko, A.; Yang, Y.; Knaust, A.; Thomas, H.; Jiang, H.; Lu, E.; Wang, C.; Shevchenko, A. *J. Proteomics* **2014**, *105*, 363–371.

(4) Solazzo, C.; Fitzhugh, W. W.; Christian, R.; Tokarski, C. *Anal. Chem.* **2008**, *80*, 4590–4597.

(5) Liu, F.; Gong, D. C. *J. Silk* **2017**, *2*, 1–5.

(6) Heginbotham, A.; Millay, V.; Quick, M. *J. Am. Inst. Conserv.* **2006**, *45*, 89–105.

(7) Zheng, Q.; Wu, X.; Zheng, H.; Zhou, Y. *Anal. Bioanal. Chem.* **2015**, *407*, 3861–3867.

(8) Cartechini, L.; Vagnini, M.; Palmieri, M.; Pitzurra, L.; Mello, T.; Mazurek, J.; Chiari, G. *Acc. Chem. Res.* **2010**, *43*, 867–876.

(9) Vagnini, M.; Pitzurra, L.; Cartechini, L.; Miliani, C.; Brunetti, B. G.; Sgamellotti, A. *Anal. Bioanal. Chem.* **2008**, *392*, 57–64.

(10) Ooi, S. Y.; Salvador, C.; Martins, S.; Pereira, A.; Caldeira, A. T.; Ramalho, J. P. *Heritage* **2019**, *2*, 2444–2456.

(11) Ooi, S. Y.; Zhang, B. J.; Yang, J. C. *Heritage* **2019**, *2*, 2444.

(12) Wu, M.; Zou, X.; Zhang, B.; Zhao, F.; Xie, Z. *Microsc. Microanal.* **2019**, *25*, 822–829.

(13) Wu, M.; Zhang, B.; Jiang, L.; Wu, J.; Sun, G. *J. Archaeol. Sci.* **2018**, *100*, 80–87.

(14) Li, J.; Zheng, H.; He, Y.; Chen, B.; Liu, L.; Ouyang, Y.; Zhu, C.; Zhou, Y.; Sun, J.; Hu, Z.; Wang, B. *ACS Sens.* **2019**, *4*, 3203–3209.

(15) Zheng, H.; Zhang, W.; Yang, H.; Ma, C.; Zhou, Y.; Dai, X. *J. Cult. Herit.* **2019**, *38*, 46–52.

(16) Chen, R.; Hu, M.; Zheng, H.; Yang, H.; Zhou, L.; Zhou, Y.; Peng, Z.; Hu, Z.; Wang, B. *Anal. Chem.* **2020**, *92*, 2435–2442.

(17) You, Q.; Liu, M.; Liu, Y.; Zheng, H.; Hu, Z.; Zhou, Y.; Wang, B. *J. Agric. Food Chem.* **2017**, *65*, 7805–7812.

(18) Zheng, H.; Yang, H.; Zhang, W.; Yang, R.; Su, B.; Zhao, X.; Zhou, Y.; Dai, X. *J. Archaeol. Sci.* **2020**, *115*, 105089.

(19) Zheng, H. L.; Ma, C.; Dai, X. J.; Zhou, Y. *Archaeometry* **2019**, *61*, 921–932.

(20) Liu, J.; Guo, D.; Zhou, Y.; Wu, Z.; Li, W.; Zhao, F.; Zheng, X. *J. Archaeol. Sci.* **2011**, *38*, 1763–1770.

(21) Akyuz, T.; Akyuz, S.; Balci, K.; Gulec, A. *J. Cult. Herit.* **2017**, *25*, 180–184.

(22) Yu, S.; Hwang, Y. H.; Hwang, J. Y.; Hong, S. H. *Compos. Sci. Technol.* **2019**, *175*, 18–27.

(23) Raneri, S.; Giannoncelli, A.; Mascha, E.; Toniolo, L.; Roveri, M.; Lazzeri, A.; Coltelli, M. B.; Panariello, L.; Lezzerini, M.; Weber, J. *Mater. Charact.* **2019**, *156*, 109853.

(24) Busto, M. D.; Perez-Mateos, M. *Eur. J. Soil Sci.* **2000**, *51*, 193–200.

(25) Doni, S.; Macci, C.; Peruzzi, E.; Ceccanti, B.; Masciandro, G. *Sci. World J.* **2014**, *2014*, 416074.

(26) Gu, J.; Xu, C.; Li, M.; Chen, B.; Shang, Y.; Zheng, H.; Zhou, Y.; Hu, Z.; Peng, Z.; Wang, B. *Anal. Sci.* **2019**, *35*, 175–180.

(27) Gu, J.; Li, Q.; Chen, B.; Xu, C.; Zheng, H.; Zhou, Y.; Peng, Z.; Hu, Z.; Wang, B. *Sci. Rep.* **2019**, *9*, 9381.

(28) Solazzo, C.; Dyer, J. M.; Clerens, S.; Plowman, J.; Peacock, E. E.; Collins, M. J. *Int. Biodeterior. Biodegrad.* **2013**, *80*, 48–59.

(29) Von Holstein, I. C. C.; Penkman, K. E. H.; Peacock, E. E.; Collins, M. J. *Rapid Commun. Mass Spectrom.* **2014**, *28*, 2121–2133.

(30) Hermes, A. C.; Davies, R. J.; Greiff, S.; Kutzke, H.; Lahlil, S.; Wyeth, P.; Riekel, C. *Biomacromolecules* **2006**, *7*, 777–783.

(31) Arai, T.; Freddi, G.; Innocenti, R.; Tsukada, M. *J. Appl. Polym. Sci.* **2004**, *91*, 2383–2390.

(32) Zeng, Y.; Peng, Z.; Wang, B.; Hu, Z.; Wan, J.; Zhou, Y. *Anal. Sci.* **2017**, *33*, 579–583.

(33) Shao, J.; Zheng, J.; Liu, J.; Carr, C. M. *J. Appl. Polym. Sci.* **2005**, *96*, 1999–2004.

(34) Zhang, S. L.; Gao, H. Y. *Cult. Relics Cent. China* **1999**, *3*, 10–16.